LETTER

doi:10.1038/nature10289

Forming the lunar farside highlands by accretion of a companion moon

M. Jutzi[1,2] & E. Asphaug[1]

The most striking geological feature of the Moon is the terrain and elevation dichotomy[1] between the hemispheres: the nearside is low and flat, dominated by volcanic maria, whereas the farside is mountainous and deeply cratered. Associated with this geological dichotomy is a compositional and thermal variation[2,3], with the nearside Procellarum KREEP (potassium/rare-earth element/phosphorus) Terrane and environs interpreted as having thin, compositionally evolved crust in comparison with the massive feldspathic highlands. The lunar dichotomy may have been caused by internal effects (for example spatial variations in tidal heating[4], asymmetric convective processes[5] or asymmetric crystallization of the magma ocean[6]) or external effects (such as the event that formed the South Pole/Aitken basin[1] or asymmetric cratering[7]). Here we consider its origin as a late carapace added by the accretion of a companion moon. Companion moons are a common outcome of simulations[8] of Moon formation from a protolunar disk resulting from a giant impact, and although most coplanar configurations are unstable[9], a ~1,200-km-diameter moon located at one of the Trojan points could be dynamically stable for tens of millions of years after the giant impact[10]. Most of the Moon's magma ocean would solidify on this timescale[11,12], whereas the companion moon would evolve more quickly into a crust and a solid mantle derived from similar disk material, and would presumably have little or no core. Its likely fate would be to collide with the Moon at ~2–3 km s^{-1}, well below the speed of sound in silicates. According to our simulations, a large moon/Moon size ratio (~0.3) and a subsonic impact velocity lead to an accretionary pile rather than a crater, contributing a hemispheric layer of extent and thickness consistent with the dimensions of the farside highlands[1,13] and in agreement with the degree-two crustal thickness profile[4]. The collision furthermore displaces the KREEP-rich layer to the opposite hemisphere, explaining the observed concentration[2,3].

A study of the evolution of a terrestrial multiple-moon system in two dimensions[9] revealed that such systems, which are assumed to have formed from impact-generated disks, are typically unstable on short ($<10^4$ yr) timescales owing to the rapid, tidally driven expansion of the Moon's orbit from its initial configuration very close to Earth. A moon that formed between Earth and the Moon might be stable for longer time, and stable three-dimensional configurations are plausible. A moon can also be trapped at one of the Earth–Moon Trojan points. Although the dynamics of large Trojan moons are complex, it was shown recently[10] that Trojans larger than 150 km in diameter can survive the Moon's orbital evolution for ~70 Myr, at which time they pass through the weak solar resonance at 27 Earth radii. Destabilized Trojans eventually collide with the Moon or Earth at a velocity close to the mutual escape velocity.

We use a smooth particle hydrodynamics (SPH) code[14,15] to simulate such collisions. For the solid components of the impactor and target, we implement[16] a rheological model for dense granular flow[17], using a block size of 5 km. For impacts, this behaves much like a Mohr–Coulomb rheology for dry friction. At global lunar scales, the hydrostatic and impact pressure forces overwhelm the rheological stresses, such that the simulation outcomes are not very sensitive to these rheological parameters; similar results are obtained using a liquid rheology throughout. We model the Moon as a 3,500-km-diameter sphere with 700-km-diameter iron core. Thermal evolution models[12] indicate that ~70 Myr after its formation, the Moon still had a small ($\lesssim$100-km-deep) magma ocean. We assume that a 50-km-deep magma ocean (modelled with a liquid rheology) remains, underneath a 20-km-thick lid of crustal composition. Although these layers are thin in comparison with the impactor diameter, and do not have a significant effect on the collisional dynamics, the magma ocean is numerically resolved in our 2,500,000-particle SPH simulations (smoothing length, $h \approx 20$ km) and the Moon's initial crust is marginally resolved. This allows us to track the dynamical evolution and redistribution of lunar material.

The companion moon, which is formed from the same protolunar disk, is similar in composition to the Moon. We model it as a 1,270-km-diameter sphere (sufficient to add 50 km of elevation to one hemisphere) consisting of lunar-like mantle below an 80-km-thick lunar-like crust. In the simulations presented here, the companion lacks an iron core; we assume that any clumps of dense iron in the protolunar disk nucleated the Moon. Simulations including a small iron core show that it sinks to join the Moon's core and does not change the overall outcome.

For the collision velocity, we assume a value of $v_{\rm imp} = 2.4$ km s^{-1}, which is 1.15 times the two-body escape velocity, $v_{\rm esc} = [2G(M_1 + M_2)/(R_1 + R_2)]^{0.5}$, where G is the gravitational constant and M_i and R_i ($i = 1, 2$) are respectively the masses and radii of the colliding bodies. In terms of the escape velocity, our impact condition is similar to the one used in the Moon-forming giant-impact simulations (see, for example, refs 18, 19), where typically $v_{\rm imp} \approx v_{\rm esc}$. However, the different impactor/target mass ratio (~1/10 in refs 18, 19 versus ~1/25 here) and, in particular, the different absolute impact velocities (10 km s^{-1} (hypervelocity) in refs 18, 19 versus 2.4 km s^{-1} (subsonic) here) indicate that these are two different types of collisions. This can also be illustrated by computing the specific incoming kinetic energy, $Q = (1/2)M_2 {v_{\rm imp}}^2/M_1$, which is ~40 times larger in the Moon-forming giant impact than in our proposed Moon–moon collision. (Here M_2 is the mass of the impactor and M_1 is the mass of the target.)

We compute self-gravity using a grid-based gravity solver. The final thermal state is important to the long-term fate of the accreted material, but because the collision is subsonic, the post-impact thermal state is for the most part advected from the pre-impact state. Impact melting is not important at these velocities, but the presence of melt within the Moon is expected during the first ~10–100 Myr (ref. 11). Both the target and the impactor are evolved to hydrostatic equilibrium in the simulation before the collision. We use the Tillotson equation of state for iron (the Moon's core) and dunite (the Moon's mantle and crust and the companion moon) (compare with ref. 20). The initial densities of the target materials are 7.8 g cm^{-3} (core), 3.4 g cm^{-3} (mantle and magma ocean) and 2.9 g cm^{-3} (crust). For the impactor, we use 3.0 g cm^{-3} (mantle) and 2.9 g cm^{-3} (crust). We consider two impact angles, 0° (head-on collision) and 45°. Because of the initial, presumably tidally locked state,

[1]Earth and Planetary Sciences Department, University of California, Santa Cruz, 1156 Highstreet, Santa Cruz, California 95060, USA. [2]Physics Institute, University of Bern, Sidlerstrasse 5, 3012 Bern, Switzerland.

we assume zero pre-impact rotation. We have not considered post-impact diffusion by short-term (viscous flow or seismic fluidization) or long-term (tidal/thermal) processes.

Our primary finding is that a companion moon ~1/3 the diameter of the Moon, striking at subsonic velocity, does not form a crater. For this low impact velocity and large impactor scale, the impactor volume, V_{imp}, exceeds the excavated volume, V_{exc}, and the impact produces an accretionary pile rather than a crater. Although our initial conditions are clearly not those that are assumed by point-source scaling laws[21], it is interesting to note that, assuming a flat geometry, the scaling laws predict that $V_{imp}/V_{exc} \approx 5$, that is, much more added material than excavated volume.

Most of the colliding material stays local to the impact (Fig. 1), pasting on a thickened crust and forming a mountainous region comparable in extent to the farside highlands. Underneath the accreted impactor, the Moon's magma ocean is displaced to the opposite hemisphere, as can be seen in cross-section in Fig. 2. As can also be seen in Figs 1 and 2, the initial crust of the impactor stays on top. According to our model, the post-impact density gradient of the hemisphere with the accreted impactor is stable.

Our choice of initial densities is based on the assumption that the impactor accreted from materials with densities no greater than that of the Moon. At ~1/10 the interior pressure of the Moon, the moon's solids would have been less compacted; the moon's mass density would also be lower if the Moon accreted around any and all iron in the disk. If the impacting moon was for some reason more dense than the Moon, then the collisional outcome and distribution of material would be about the same, but the resulting structure might be unstable in the long term, resulting in a denser hemispheric pancake of material that might

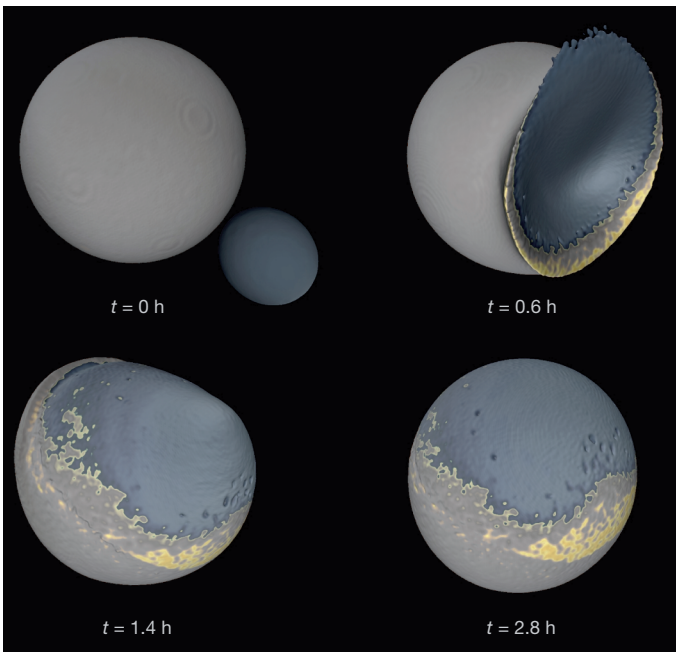

Figure 1 | Moon/companion moon collision. We use SPH to simulate collisions between the Moon and a companion moon, ~4% the lunar mass, dislodged from one of the Earth–Moon Trojan points, to explore whether the Moon's farside highlands and its nearside KREEP-rich terrain can be explained by this late, slow accretion. Snapshots (t, simulation time) show the case of a 2.4 km s^{-1}, 45° impact of a 1,270-km-diameter Trojan moon impacting the 3,500-km-diameter Moon. Plotted is an iso-density surface $\rho_{iso} = 2$ g cm^{-3}; lower density materials are invisible. Plotted colours indicate impactor crust (light blue), impactor mantle (dark blue), target crust (grey) and a layer of target upper mantle material (yellow) representing a magma ocean. Most of the impactor is accreted as a pancake-shaped layer, forming a mountainous region comparable in extent to the lunar farside highlands. A residual magma ocean, if present, gets pushed (Fig. 2) to the opposite hemisphere.

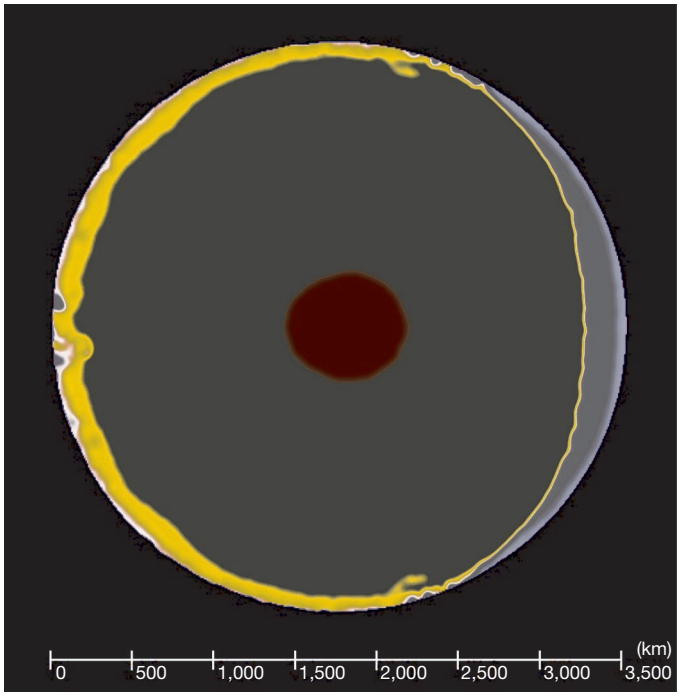

Figure 2 | Post-impact internal structure. Two-dimensional view of the post-impact distribution of layers of target and impactor materials for the case of the head-on impact simulation. The companion moon collided from the right, accreting as a pile and producing the farside lunar highlands in our model. Grey and light blue correspond to the mantle and crust of the companion moon, respectively. The initially global residual magma ocean (yellow) is displaced to the opposite hemisphere, leading to an asymmetric distribution of KREEP. The initial ~20-km-thick crust of the target (white) is poorly resolved in the code, and not shown to scale.

founder. Although this could provide another explanation of hemispheric dichotomy, we consider the more reasonable picture of a companion moon no denser than the Moon, and consequently stable layering.

The impacting moon, forming in the same giant impact event as the Moon but solidifying more rapidly in a smaller sized body, has an older crust. Our model therefore predicts two differing ages for lunar anorthositic crustal rocks. A fraction of the older crust (from the impactor) ends up on the nearside in the 45° impact simulation (Fig. 3), and we expect further widespread redistribution of crustal material following subsequent basin-forming events. Measured lunar crustal ages do show a wide spread[11] (~200 Myr), which is consistent with our picture of two compositionally similar crustal reservoirs.

In Fig. 3, we plot the post-impact thickness of the accreted moon material in a cylindrical projection of the Moon. For both impact angles considered here, the resulting pancake of material is comparable in extent to the farside highlands. A profile of the resulting crustal thickness for latitude 0° is also shown in Fig. 3. In the impacted hemisphere, our result can be very well fitted by a degree-two Legendre polynomial. Although our model reproduces the observed degree-two terrain well, other geological mechanisms can in principle also lead to similar terrain forms. For instance, the degree-two terrain has been interpreted[4] as evidence for spatial variation in tidal heating. The near-side would in that case require a second major event or a process of crustal thinning. In our model, the accretion of a large impactor is shown to result in a highlands region with a degree-two thickness structure, in accordance with the observations, and only on the impacted hemisphere.

Our resulting degree-two terrain profiles have amplitudes greater than the observed variations in crustal thickness[1,4,13]. A comprehensive analysis of our simulation results would use the density structure of the

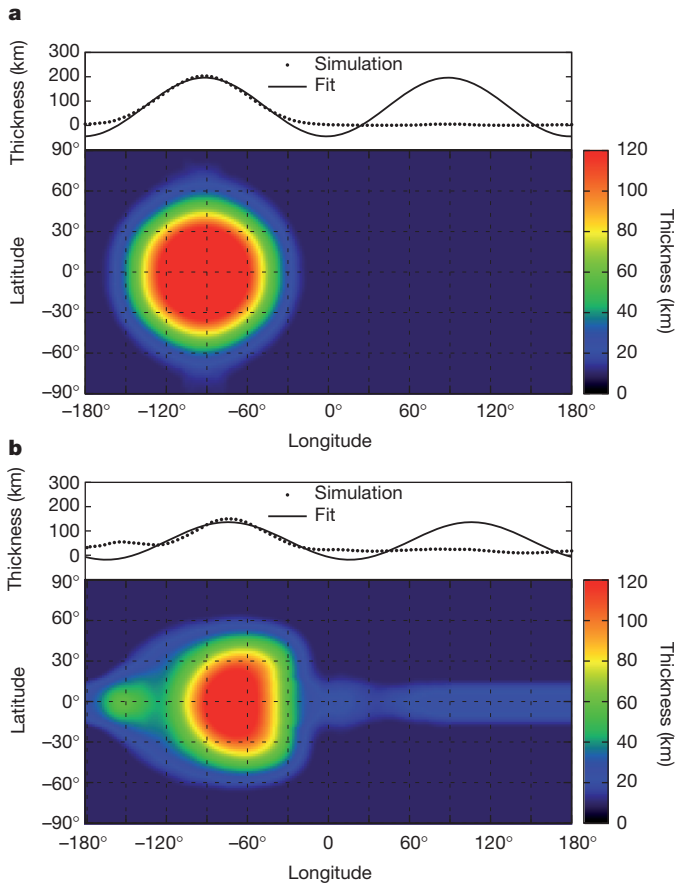

Figure 3 | Post-impact spatial distribution of the impactor and thickness profile. Thickness of the impactor layer accreted onto the Moon, shown as a function of longitude (−180° to 180°) and latitude (−90° to 90°), after a 1,270-km-diameter moon impacts at 2.4 km s^{-1}: head-on impact (**a**), 45° impact from the right (**b**). The 'bull's-eye' would be the lunar farside. Also shown are a thickness profile computed for the great circle at latitude 0° and, for comparison, a degree-two Legendre polynomial that was fitted to the thickness profile.

accreted impactor on the Moon to compute a modelled post-impact Bouguer gravity anomaly, for direct comparison with observations[1]. Such a detailed gravity and terrain comparison is complicated because we must assume a pre-impact structure for the Moon and to be accurate must resolve the Moon's crust at the time of impact using three to five particles, requiring ~10^8 particle simulations and much faster computation. Perhaps more importantly, the post-impact shape may not be well preserved if the Moon is still significantly molten.

KREEP is found concentrated in the Procellarum KREEP Terrane, one of the three major geologic provinces of the Moon[3], situated on the nearside. According to the magma ocean model[22], the incompatible elements of which it is composed (potassium, phosphorus and the rare-earth elements) are concentrated in the last magmas to crystallize and are sandwiched between the floating anorthositic crust and the mantle cumulates. In some models[23], the Moon's KREEP asymmetry is explained as a result of a degree-one Rayleigh–Taylor instability. Our model provides an alternative explanation. This is illustrated in Fig. 2, where the magma ocean at the time of the impact (the global liquid layer) is pushed/ejected to the opposite hemisphere in response to the same forces that flatten and accrete the impactor.

One obvious test of our model would be to determine whether there is evidence of accretion of a foreign-composition body on the Moon's farside. However, the companion moon formed from the same protolunar disk as the Moon, evolved similarly (although faster, being smaller) and was not shocked by the final collision, so we expect compositional distinctions to be subtle. A more important test will be to compare the lunar farside with the high-definition gravimetric determinations of the crust and mantle in the upcoming data sets from the NASA Gravity Recovery and Interior Laboratory mission[24], and others, and perhaps more clearly in forthcoming lunar seismology experiments. In particular, if the KREEP was actually pushed from one hemisphere to the other, this deep-scale evolution should be preserved. Finally, we should acknowledge that although the dynamical modelling[10] indicates the possibility of a Trojan moon surviving for tens of millions of years, there is much work to be done studying the long-term after-effects of Moon-forming giant impacts.

METHODS SUMMARY

We use an SPH impact code[14,15] specially written to model geologic materials. Our code computes the full stress tensor, $\sigma_{ij} = -P\delta_{ij} + \tau_{ij}$, where P denotes pressure, δ_{ij} is the Kronecker delta function and τ_{ij} is the deviatoric stress tensor. For solids, we apply a model for dense granular flow[17] that has a Drucker–Prager-like yield criterion: material flows only if $|\tau| > \mu_s P$, where $|\tau|$ is the second invariant of τ_{ij} and $\mu_s = 0.7$ is the static friction coefficient. A yield stress of P or 0.1 GPa, whichever is the lesser, is applied to the computation of σ_{ij}, and tensile strength is neglected in these simulations. Comparison simulations using a liquid rheology showed no significant differences in terms of the final distribution of impactor material. Self-gravity is computed using a grid-based solver. Both the target and the impactor are evolved to hydrostatic equilibrium before the collision. The initial separation between the impactor and the target is one target radius; the impactor is assigned an initial velocity of 1.8 km s^{-1}, which leads to an impact velocity of 2.4 km s^{-1}. The collision simulations are carried out over a simulation time of ~10 h, which takes about seven days on 32 computer processors for a resolution of 2.5×10^6 SPH particles.

Received 8 April; accepted 13 June 2011.

1. Zuber, M. T., Smith, D. E., Lemoine, F. G. & Neumann, G. A. The shape and internal structure of the moon from the Clementine mission. *Science* **266,** 1839–1843 (1994).
2. Lawrence, D. J. Global elemental maps of the moon: the Lunar Prospector gamma-ray spectrometer. *Science* **281,** 1484–1489 (1998).
3. Jolliff, B. L., Gillis, J. J., Haskin, L. A., Korotev, R. L. & Wieczorek, M. A. Major lunar crustal terranes: surface expressions and crust-mantle origins. *J. Geophys. Res.* **105,** 4197–4216 (2000).
4. Garrick-Bethell, I., Nimmo, F. & Wieczorek, M. Structure and formation of the lunar farside highlands. *Science* **330,** 949–951 (2010).
5. Loper, D. E. & Werner, C. L. On lunar asymmetries 1. Tilted convection and crustal asymmetry. *J. Geophys. Res. Planets* **107,** 131–137 (2002).
6. Wasson, J. T. & Warren, P. H. Contribution of the mantle to the lunar asymmetry. *Icarus* **44,** 752–771 (1980).
7. Wood, J. A. Bombardment as a cause of the lunar asymmetry. *Moon* **8,** 73–103 (1973).
8. Ida, S., Canup, R. M. & Stewart, G. R. Lunar accretion from an impact-generated disk. *Nature* **389,** 353–357 (1997).
9. Canup, R. M., Levison, H. F. & Stewart, G. R. Evolution of a terrestrial multiple-moon system. *Astron. J.* **117,** 603–620 (1999).
10. Cuk, M. & Gladman, B. J. The fate of primordial lunar Trojans. *Icarus* **199,** 237–244 (2009).
11. Elkins-Tanton, L. T., Burgess, S. & Yin, Q.-Z. The lunar magma ocean: reconciling the solidification process with lunar petrology and geochronology. *Earth Planet. Sci. Lett.* **304,** 326–336 (2011).
12. Meyer, J., Elkins-Tanton, L. & Wisdom, J. Coupled thermal–orbital evolution of the early moon. *Icarus* **208,** 1–10 (2010).
13. Wieczorek, M. The constitution and structure of the lunar interior. *Rev. Mineral. Geochem.* **60,** 221–364 (2006).
14. Benz, W. & Asphaug, E. Simulations of brittle solids using smooth particle hydrodynamics. *Comput. Phys. Commun.* **87,** 253–265 (1995).
15. Jutzi, M., Benz, W. & Michel, P. Numerical simulations of impacts involving porous bodies. I. Implementing sub-resolution porosity in a 3D SPH hydrocode. *Icarus* **198,** 242–255 (2008).
16. Jutzi, M. & Asphaug, E. Mega-ejecta on asteroid Vesta. *Geophys. Res. Lett.* **38,** L01102 (2011).
17. Jop, P., Forterre, Y. & Pouliquen, O. A constitutive law for dense granular flows. *Nature* **441,** 727–730 (2006).
18. Benz, W. The origin of the moon and the single-impact hypothesis. I. *Icarus* **66,** 515–535 (1986).
19. Canup, R. M. & Asphaug, E. Origin of the Moon in a giant impact near the end of the Earth's formation. *Nature* **412,** 708–712 (2001).
20. Melosh, H. J. *Impact Cratering: A Geologic Process* (Oxford Univ. Press, 1989).
21. Housen, K. R., Schmidt, R. M. & Holsapple, K. A. Crater ejecta scaling laws: fundamental forms based on dimensional analysis. *J. Geophys. Res.* **88,** 2485–2499 (1983).
22. Warren, P. H. The magma ocean concept and lunar evolution. *Annu. Rev. Earth Planet. Sci.* **13,** 201–240 (1985).

23. Parmentier, E. M., Zhong, S. & Zuber, M. T. Gravitational differentiation due to initial chemical stratification: origin of lunar asymmetry by the creep of dense KREEP? *Earth Planet. Sci. Lett.* **201,** 473–480 (2002).
24. Zuber, M. T. *et al.* in *Proc. 39th Lunar Planet. Sci. Conf.* abstr. 1074, ⟨http://www.lpi.usra.edu/meetings/lpsc2008/pdf/1074.pdf⟩ (Lunar and Planetary Institute, 2008).

Acknowledgements Our work is sponsored by NASA's Planetary Geology and Geophysics programme 'Small Bodies and Planetary Collisions'. All simulations were run at the University of California, Santa Cruz, on the NSF-MRI-sponsored 'pleiades' cluster. We are grateful to M. Cuk, B. Gladman and R. Canup for guidance.

Author Contributions Both authors contributed equally to this work.

Author Information Reprints and permissions information is available at www.nature.com/reprints. The authors declare no competing financial interests. Readers are welcome to comment on the online version of this article at www.nature.com/nature. Correspondence and requests for materials should be addressed to M.J. (martin.jutzi@space.unibe.ch).